JACS
JOURNAL OF THE AMERICAN CHEMICAL SOCIETY
Communication
pubs.acs.org/JACS

Large Area Synthesis of a Nanoporous Two-Dimensional Polymer at the Air/Water Interface

Daniel J. Murray,[†] Dustin D. Patterson,[†] Payam Payamyar,[‡] Radha Bhola,[†] Wentao Song,[§,∥] Markus Lackinger,[§,∥] A. Dieter Schlüter,[‡] and Benjamin T. King*[,†]

[†]Department of Chemistry, University of Nevada, Reno, Nevada 89557-0216, United States

[‡]Laboratory of Polymer Chemistry, Institute of Polymers, Department of Materials, ETH Zürich, Vladimir-Prelog-Weg 5, CH-8093 Zürich, Switzerland

[§]Department of Physics, Technische Universität München, James-Franck-Str. 1, 85748 Garching, Germany

[∥]Deutsches Museum, Museumsinsel 1, 80538 Munich, Germany

Supporting Information

ABSTRACT: We present the synthesis of a two-dimensional polymer at the air/water interface and its nm-resolution imaging. Trigonal star, amphiphilic monomers bearing three anthraceno groups on a central triptycene core are confined at the air/water interface. Compression followed by photopolymerization on the interface provides the two-dimensional polymer. Analysis by scanning tunneling microscopy suggests that the polymer is periodic with ultrahigh pore density.

The synthesis of two-dimensional polymers (2DPs) allows for structural control that might enable application in surface patterning,[1,2] molecular electronics,[3,4] van der Waals heterostructures,[5] and, most notably to us, hyperthin membranes for separations.[6,7] Extensive reviews of 2DPs have appeared recently.[8,9] King and co-workers defined[10] 2DPs as tilings, where the repeat units are the vertices and their connections are edges. These edges outline tiles that completely cover the plane without gaps or overlaps. For example, in graphene, the C atoms are the repeat units, the C−C bonds are the edges, and the edges outline hexagons that cover the plane. This definition emphasizes the characteristic two-dimensionality that distinguishes 2DPs from other thin materials.

Many 2DPs are prepared by the exfoliation of lamellar, three-dimensional crystals. The exfoliation of graphite to graphene[11] is the prototypical example. Other examples of 2DPs prepared in this way include hexagonal boron nitride,[12] transition metal dichalcogenides,[13] layered covalent− and metal−organic frameworks,[14] and layered organic crystals.[10,15−17] The preparation of sheets sufficiently large for applications remains a challenge because 2DPs from crystal exfoliation are small, commonly ranging from 0.5 to 3 μm on a side. The production of devices utilizing 2DPs will require large sheets.[18] For this reason, we explore preorganization and polymerization of monomers at the air/water interface to provide sheets on the cm^2 scale.

2DPs might enable desalination technology to ameliorate the global water crisis.[19,20] Molecular dynamics studies of hyperthin, porous membranes suggest that such membranes can provide fluxes that are 2 to 3 orders of magnitude higher than conventional membranes.[21,22] Separations based on molecular size (molecular sieving) require precisely defined pores with a narrow size distribution. An ideal membrane could reduce the size and capital costs of a desalination plant by two- to three-orders of magnitude and operate near the thermodynamic limit of efficiency.[23]

We report herein a synthetic 2DP, prepared on the macroscopic scale (cm^2), that is thin (1.2 nm), porous (6.8×10^{13} pores/cm^2, ∼30% open area), sufficiently strong to support itself in an open atmosphere, and stable to hydrolysis.

We use the air/water interface to constrain monomers to two dimensions during polymerization. This approach is not new. Indeed, Gee reported the polymerization of β-elaeostearin at the air/water interface in 1935.[24]

Regan has performed extensive work on the polymerization of calix[n]arenes at this interface and their subsequent use in molecular sieving.[25−27] Schlüter recently showed an anthracene containing monolayer sheet made at the air/water interface having the strength to span 20 μm × 20 μm holes.[28] Other notable contributions in this field have been made by Kunitake[29] and Barraud.[30] Similarly, Michl has made strides toward a 2DP at the air/mercury interface.[31]

Our 2DP is prepared from antrip-DEG (Figure 1a), a rigid, amphiphilic monomer consisting of three anthraceno blades organized on a central triptycene core that has a diethylene glycol tail at one bridgehead. The diethylene glycol chain

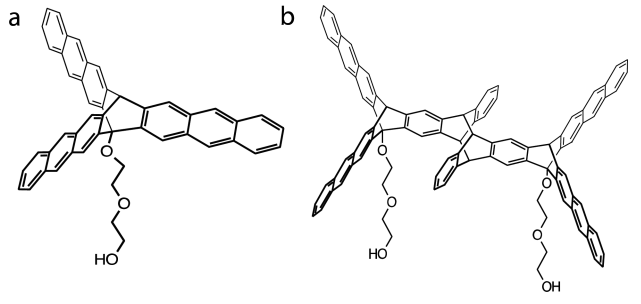

Figure 1. Structure of antrip-DEG and its photodimer.

Received: November 24, 2014
Published: February 26, 2015

DOI: 10.1021/ja512018j
J. Am. Chem. Soc. 2015, 137, 3450−3453

anchors the monomer to the water surface with the antrip body lying on the interface. Monomers link via dimerization of the anthraceno blades (Figure 1b). This design is an extension of the antrip monomer previously developed in our laboratories for 2DPs generated by photopolymerization in the crystal state.[10,16] By extension, we hypothesized that irradiation of a compressed monolayer of antrip-DEG on the interface should afford the 2DP as a large, single sheet.

Antrip-DEG was synthesized starting from 9-methoxyanthracene in eight steps. The route (see Supporting Information (SI) for synthetic details) afforded sufficient quantities of material for all experiments. The full details of the synthesis and its optimization will be published separately.

An antrip-DEG solution was spread at the air/water interface in a Langmuir–Blodgett trough. Compression isotherms (Figure 2) at 1 °C exhibited a phase change at about 155–

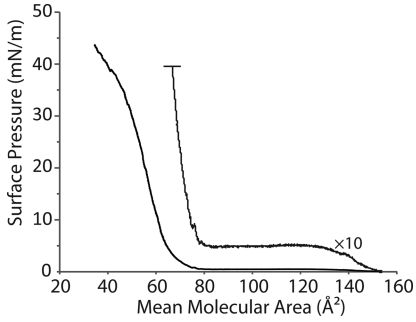

Figure 2. Isotherm of antrip-DEG at 1 °C spread from a 0.5 mg/mL solution in 1:1 $CHCl_3$/cyclohexane.

135 Å^2/molecule and a second at ~80 Å^2/molecule. This first phase change was not observed at 25 °C (Figure S3). The mean molecular area (MMA) of the low-pressure transition suggests the initial formation of a hexagonal *p6* packing (Figure S11), a motif also observed in crystal packing of a fluorinated analog.[16] We would expect an MMA of 155 Å^2 for this packing. Upon further compression, this lattice collapses to a more dense packing.

The structure of the dense packing is not obvious. The maximally dense packing for a trigonal star is the lattice shown in Figure S13 and suggests an MMA of about 100 Å^2, which is significantly higher than we observe. It is not uncommon, however, for extended molecules to give a smaller MMA than would be expected.[32] Because we are interested in the less dense, and thus porous, *p6* packing, the subsequent experiments are of films made at 1 °C and 0.5 mN/m.

The compression process was also followed by Brewster angle microscopy (Figure S4). Aggregation into large domains with few defects was observed upon initial spreading at 1 °C, and these domains then coalesced into a homogeneous film upon compression to 0.5 mN/m. Once the film is compressed beyond 0.5 mN/m, a higher contrast in the film was observed. This is consistent with the initial formation of a loose packing that rearranges to a tight packing upon compression.

The compressed film (1 °C, 0.5 mN/m, 150 Å^2/molecule) was photopolymerized at the air/water interface using 365 nm light (see SI for details). Attempts to measure the postpolymerization molecular area were impossible because the rigid 2DP could not be reversibly compressed. Indeed, the 2DP on water was sufficiently rigid to force the paper Wilhemy plate out of vertical alignment by up to ~30° when a single barrier trough was used (Figure S17).

These poly(antrip-DEG) films can be transferred from the interface to a variety of substrates. Transfer to a TEM grid by the Langmuir–Schaefer method and subsequent imaging by optical microscopy (OM) reveals that the 2DP is free-standing. Figure 3a shows a reflected polarized optical microscopy

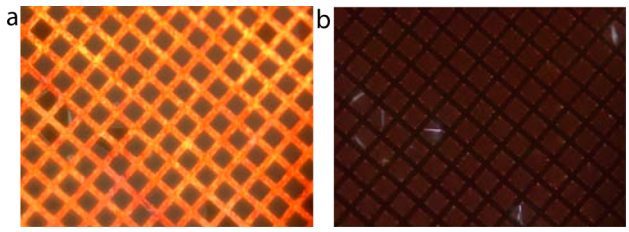

Figure 3. (a) Polarized reflectance optical microscopy image of polymerized film spanning 20 × 20 μm^2 holes on a TEM grid. (b) Crossed polarized optical microscopy image of the same area as image a.

(POM) image of the TEM grids with poly(antrip-DEG) spanning 20 μm × 20 μm holes. A few tears are evident and likely form during transfer. Crossed polarizers (Figure 3b) reveal that these tears, in which the 2DP is no longer perpendicular to the optical axis, are birefringent. Nonetheless, pristine 1 mm^2 areas of unbroken 2DP are commonly obtained. A control experiment without irradiation fails to produce a freestanding film.

Transfer by the Langmuir–Blodgett method to SiO_2 wafers allows for imaging by reflectance POM and atomic force microscopy (AFM). Long (mm), straight edges and cracks are observed by reflectance POM (Figure 4a), indicating that the

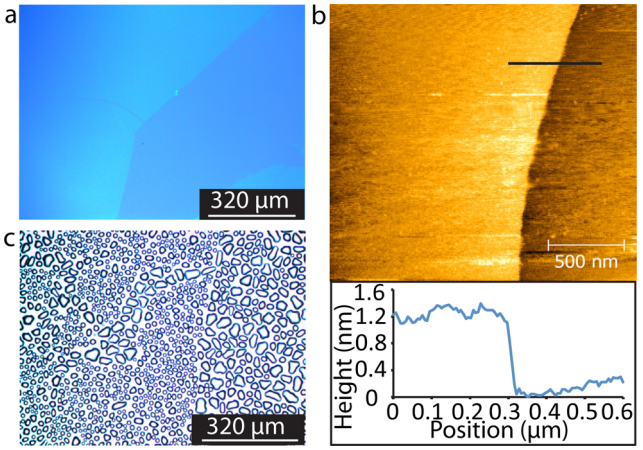

Figure 4. (a) OM image of poly(antrip-DEG) on SiO_2. (b) AFM height image of poly(antrip-DEG) on SiO_2 with the height profile along the black line. (c) Water condensation on a SiO_2 wafer partly coated with poly(antrip-DEG). Large droplets show uncoated SiO_2, and small droplets reveal the coated portion.

2DP breaks along cleavage lines. AFM imaging (Figure 4b) of single layer polymer films on SiO_2 reveals a thickness of ~1.2 nm, which is consistent with the expected height of a monolayer. This thickness is constant over large areas. 2DP sheets covering ~1 cm^2 have been transferred onto SiO_2 wafers (Figure S18).

DOI: 10.1021/ja512018j
J. Am. Chem. Soc. 2015, 137, 3450–3453

The contact angle of water on a single layer of poly(antrip-DEG) on SiO_2 (Figure S16) is 92°, which is comparable to conventional self-assembled monolayers containing aromatic moieties.[33] This angle indicates that the hydrophobic face of poly(antrip-DEG) faces out, as is expected from the direction of transfer off the interface. The unmasked SiO_2 has a contact angle of 50°. This difference in hydrophobicity enables visualization by water condensation (Figure 4c),[34] with larger droplets forming on uncoated SiO_2 and smaller droplets forming on 2DP-coated SiO_2. The effect is evident to the naked eye and may permit imaging of 2DPs on other supports.

Polymerization via anthracene dimers is supported by UV−vis spectroscopy. Transfer of the nonpolymerized and polymerized films onto quartz slides permitted their spectra to be obtained. The changes upon polymerization[10] (Figure S6) are similar to those observed upon polymerization of crystalline antrip.

Scanning tunneling microscopy (STM) establishes the structure of the poly(antrip-DEG) 2DP. STM imaging (Figure 5a) of the 2DP reveals a porous structure that is consistent with

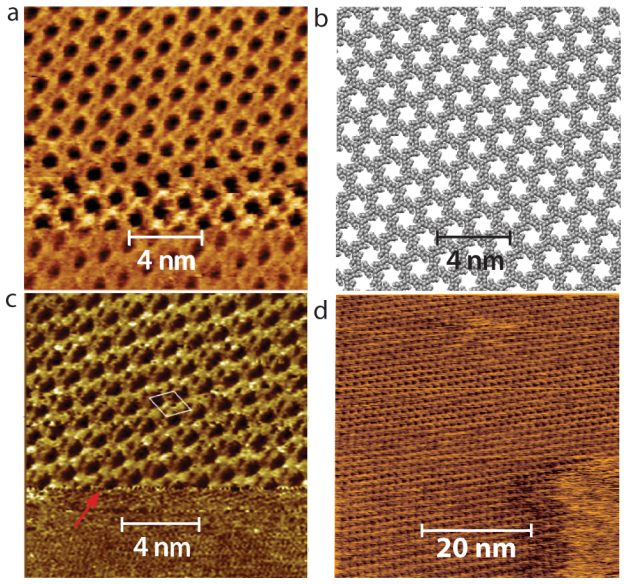

Figure 5. (a) STM image (+ 0.91 V, 28 pA) of poly(antrip-DEG) on HOPG. (b) Simulated poly(antrip-DEG) *p6* lattice at the same scale as image a. (c) Split image of monolayer poly(antrip-DEG) on HOPG showing both the 2DP lattice and the underlying HOPG lattice; the arrow marks the scan-line where the imaging parameters were changed. (d) Wide view STM image (+1.0 V, 25 pA) of poly(antrip-DEG) on HOPG under 1-phenyloctane showing a domain edge at the lower right corner.

the structure established by crystallography for related 2DPs.[16] A split-image is shown in Figures 5c and, at higher resolution, S9. In the upper part of the frame the 2DP was imaged, and at the scan-line marked by the arrow the tunneling parameters were abruptly changed during the scan for imaging the underlying HOPG in the lower part. This split-image scan demonstrates that the 2DP lattice image is real and not an artifact arising from a tip defect that gives a distorted image of the HOPG lattice. The assertion that the 2DP images are real is further supported by the observation of domain boundaries (Figure 5d). Other STM images (Figure S10) of the 2DP, albeit of lower quality, were acquired in a different laboratory.

The observed unit cell parameters (calibrated from the split image) are $a = 1.3 \pm 0.2$ nm and $b = 1.3 \pm 0.2$ nm with $\gamma = 63.5°$. This lattice constant is, however, smaller than the 1.8 nm expected from the simulated hexagonal *p6* lattice shown in Figure 5b. The origin of this difference remains unclear. The structure might be subtly different from our expectations. For example, anthracene dimerization can occur between the 1,4 and 9,10 positions (Figure S14), as has been observed in constrained anthracene−anthracene systems.[35] This linkage would give a lattice constant of 1.54 nm (Figure S15), which is within the uncertainty of these STM distance measurements. Or perhaps the lattice contracts by some deformation or distortion when mounted on the surface. Nonetheless the important conclusion remains unchanged: the amphiphilic poly(antrip-DEG) 2DP forms a porous, honeycomb lattice.

The pore density of this 2DP is enormous: $\sim 6.8 \times 10^{13}$ pores/cm^2. This is about 2 orders of magnitude higher than that reported for state of the art carbon nanotube membranes[36] and 5 orders of magnitude larger than polycarbonate track etched membranes with 10 nm pores.[36] Moreover, this 2DP is 3 orders of magnitude thinner than the carbon nanotube membranes. STM imaging indicates that the pores have a narrow size distribution and are measured to be ∼0.7 nm in diameter. The monodisperse, subnanometer pore size and monolayer thinness suggest that this 2DP might be useful in separations.

To conclude, we have prepared a 2DP by photopolymerization of antrip-DEG at the air/water interface. BAM imaging during the Langmuir−Blodgett compression shows that homogeneous monomer films can be formed. UV light irradiation of these films over the entire trough (∼50 cm^2) induces polymerization. The resulting 2DP can be transferred to both solid substrates, where cm^2 areas can be covered, and open lattices, where 20 μm × 20 μm holes can be spanned. The formation of a monolayer is confirmed by AFM. STM imaging shows that the polymer is periodic with a honeycomb lattice. We have observed boundaries by STM and suspect that the 2DP sheets comprise many domains.

■ ASSOCIATED CONTENT

Ⓢ Supporting Information

Synthetic and experimental methods, supplementary figures. This material is available free of charge via the Internet at http://pubs.acs.org

■ AUTHOR INFORMATION

Corresponding Author

*king@chem.unr.edu

Notes

The authors declare no competing financial interest.

■ ACKNOWLEDGMENTS

This work was supported by the U.S. National Science Foundation (CHE-09567702). The authors thank Dr. Carey Johnson for assistance with modeling.

■ REFERENCES

(1) Gross, A. J.; Nock, V.; Polson, M. I. J.; Alkaisi, M. M.; Downard, A. J. *Angew. Chem., Int. Ed.* **2013**, 10261.

(2) Jester, S.-S.; Sigmund, E.; Höger, S. *J. Am. Chem. Soc.* **2011**, *133*, 11062.

(3) Taylor, D. M.; Morgan, H.; D'Silva, C. *Makromol. Chem. Macromol. Symp.* **1991**, *46*, 1.

DOI: 10.1021/ja512018j
J. Am. Chem. Soc. 2015, 137, 3450−3453

(4) Yang, X.; Zhu, J.; Qiu, L.; Li, D. *Adv. Mater.* **2011**, *23*, 2771.
(5) Geim, A. K.; Grigorieva, I. V. *Nature* **2013**, *499*, 419.
(6) McCullough, D. H., III; Regen, S. L. *Chem. Commun.* **2004**, 2787.
(7) O'Hern, S. C.; Stewart, C. A.; Boutilier, M. S. H.; Idrobo, J.-C.; Bhaviripudi, S.; Das, S. K.; Kong, J.; Laoui, T.; Atieh, M.; Karnik, R. *ACS Nano* **2012**, *6*, 10130.
(8) Sakamoto, J.; van Heijst, J.; Lukin, O.; Schlüter, A. D. *Angew. Chem., Int. Ed.* **2009**, *48*, 1030.
(9) Colson, J. W.; Dichtel, W. R. *Nat. Chem.* **2013**, *5*, 453.
(10) Bhola, R.; Payamyar, P.; Murray, D. J.; Kumar, B.; Teator, A. J.; Schmidt, M. U.; Hammer, S. M.; Saha, A.; Sakamoto, J.; Schlüter, A. D.; King, B. T. *J. Am. Chem. Soc.* **2013**, *135*, 14134.
(11) Novoselov, K. S.; Geim, A. K.; Morozov, S. V.; Jiang, D.; Zhang, Y.; Dubonos, S. V.; Grigirieva, I. V.; Firsov, A. S. *Science* **2004**, *306*, 666.
(12) Lin, Y.; Connell, J. W. *Nanoscale* **2012**, *4*, 6908.
(13) Chhowalla, M.; Shin, H. S.; Eda, G.; Li, L.-J.; Loh, K. P.; Zhang, H. *Nat. Chem.* **2013**, *5*, 263.
(14) Berlanga, I.; Ruiz-González, M. L.; González-Calbet, J. M.; Fierro, J. L. G.; Mas-Ballesté, R.; Zamora, F. *Small* **2011**, *7*, 1207.
(15) Kissel, P.; Erni, R.; Schweizer, W. B.; Rossell, M. D.; King, B. T.; Bauer, T.; Götzinger, S.; Schlüter, A. D.; Sakamoto, J. *Nat. Chem.* **2012**, *4*, 287.
(16) Kissel, P.; Murray, D. J.; Wulftange, W. J.; Catalano, V. J.; King, B. T. *Nat. Chem.* **2014**, *6*, 774.
(17) Kory, M. J.; Wörle, M.; Weber, T.; Payamyar, P.; van de Poll, S. W.; Dshemuchadse, J.; Trapp, N.; Schlüter, A. D. *Nat. Chem.* **2014**, *6*, 779.
(18) Li, X.; Cai, W.; An, J.; Kim, S.; Nah, J.; Yang, D.; Piner, R.; Velamakanni, A.; Jung, I.; Tutuc, E.; Banerjee, S. K.; Colombo, L.; Ruoff, R. S. *Science* **2009**, *324*, 1312.
(19) Service, R. F. *Science* **2006**, *313*, 1088.
(20) Elimelech, M.; Phillip, W. A. *Science* **2011**, *333*, 712.
(21) Wang, E. N.; Karnik, R. *Nat. Nanotechnol.* **2012**, *7*, 552.
(22) Cohen-Tanugi, D.; Grossman, J. C. *Nano Lett.* **2012**, *12*, 3602.
(23) Cohen-Tanugi, D.; McGovern, R. K.; Dave, S. H.; Lienhard, J. H.; Grossman, J. C. *Energy Env. Sci.* **2014**, *7*, 1134.
(24) Gee, G.; Rideal, E. K. *Proc. R. Soc. Math. Phys. Eng. Sci.* **1935**, *153*, 116.
(25) Markowitz, M. A.; Bielski, R.; Regen, S. L. *J. Am. Chem. Soc.* **1988**, *110*, 7545.
(26) Markowitz, M. A.; Janout, V.; Castner, D. G.; Regen, S. L. *J. Am. Chem. Soc.* **1989**, *111*, 8192.
(27) Yan, X.; Janout, V.; Hsu, J. T.; Regen, S. L. *J. Am. Chem. Soc.* **2002**, *124*, 10962.
(28) Payamyar, P.; Kaja, K.; Ruiz-Vargas, C.; Stemmer, A.; Murray, D. J.; Johnson, C. J.; King, B. T.; Schiffmann, F.; VandeVondele, J.; Renn, A.; Götzinger, S.; Ceroni, P.; Schütz, A.; Lee, L.-T.; Zheng, Z.; Sakamoto, J.; Schlüter, A. D. *Adv. Mater.* **2014**, *26*, 2052.
(29) Kunitake, T. *Macromol. Symp.* **1995**, *98*, 45.
(30) Porteu, F.; Palacin, S.; Ruaudel-Teixier, A.; Andre, B. *Makromol. Chem. Macromol. Symp.* **1991**, *46*, 37.
(31) Michl, J.; Magnera, T. F. *Proc. Natl. Acad. Sci. U.S.A.* **2002**, *99*, 4788.
(32) Ulman, A. *An introduction to ultrathin organic films: from Langmuir-Blodgett to self-assembly*; Academic Press: Boston, 1991.
(33) Fox, M. A.; Wooten, M. D. *Langmuir* **1997**, *13*, 7099.
(34) Gonçalves, H.; Belsley, M.; Moura, C.; Stauber, T.; Schellenberg, P. *Appl. Phys. Lett.* **2010**, *97*, 231905.
(35) Bouas-Laurent, H.; Castellan, A.; Daney, M.; Desvergne, J. P.; Guinand, G.; Marsau, P.; Riffaud, M. H. *J. Am. Chem. Soc.* **1986**, *108*, 315.
(36) Holt, J. K.; Park, H. G.; Wang, Y.; Stadermann, M.; Artyukhin, A. B.; Grigoropoulos, C. P.; Noy, A.; Bakajin, O. *Science* **2006**, *312*, 1034.

DOI: 10.1021/ja512018j
J. Am. Chem. Soc. 2015, 137, 3450−3453